Numerical Prediction of Aerodynamic Performance for Low Reynolds Number Airfoils

Fie-Bin Hsiao* and Cheng-Chaing Hsu†
National Cheng Kung University, Tainan, Taiwan, Republic of China

Nomenclature

C = chord length
C_l, C_p = coefficient of lift, pressure
H = shape factor
ℓ_1, ℓ_2 = length of laminar, turbulent portion of bubble
Re_c = Reynolds number (Uc/ν)
U, V = streamwise, transverse velocity
X, Y = streamwise, transverse direction
α = angle of attack
Γ = strength of circulation
Δt = increment of time
θ = momentum thickness
λ = pressure gradient parameter $\left(\frac{\theta^2}{\nu}\frac{dU}{dx}\right)_s$
ν = kinematic viscosity
ϕ = velocity potential

Subscripts
e = tangential component
i = neighboring turbulent separation point
R,S,T = reattachment, separation, transition point of boundary layer
∞ = freestream

Introduction

BECAUSE of the large number of systems operating in a low Reynolds number range ($10^4 < Re_c < 10^6$), there is considerable importance in studying the aerodynamic performance in that range. For a low Reynolds number flow about a two-dimensional airfoil (see Fig. 1), the boundary layer developed on the surface may result in laminar separation at some distance downstream from the leading edge. It then becomes turbulent after reattaching to the surface, and possibly has a turbulent separation point near the trailing edge. In this Reynolds number range, the aerodynamic performance is affected primarily due to the existence of a bubble located between the laminar separation and reattachment points.

Since Horton[1] introduced a semiempirical method for calculating the bubble properties, low Reynolds number aerodynamics has either used Horton's theory or a modified form. Roberts[2] and Cotton and Galbraith[3] have successfully modified the theory for predicting bubble formation, which agreed with experimental results. In order to simplify the computations, the present paper employs Horton's theory only in predicting bubble formation.

It is known that the potential solution for a two-dimensional airfoil becomes incorrect when the flow separates at a high angle of attack. One reason is that the wake effect is not considered. In order to obtain a more accurate solution, Basu and Hancock,[4] as well as Kim and Mook,[5] obtained unsteady potential solutions by using discrete vortices to simulate the wake effect of an unsteady airfoil in incompressible flow. Katz[6] also employed the vortex model combined with thin airfoil theory to study the stall effect on aerodynamic performance. The cases they studied included either turbulent separation or detailed pressure distribution. In the wake model here, one releases the point vortices from the turbulent separation point and the trailing edge to improve the potential solution according to the model proposed by Sears.[7] Also, the method introduced by Blaslovich[8] is adopted to modify the pressure distribution in the region after turbulent separation point. This technique is not only quite simple and efficient but is also reasonably accurate, as verified by experimental results.

Preliminary Prediction Method

The panel method[9] was first used to solve the potential flow equation for NACA 63_3-018 and 66_3-018 airfoils. Since the calculated Reynolds number is greater than 10^5, the flowfield over the airfoil may already be separated. The flow properties related to the separation are the boundary-layer development, the laminar separation point, transition, reattachment point, and the turbulent separation point. The information about the boundary-layer development can be obtained by Thwaits' method[10] for the laminar portion. The Michel's criteria[9] are then used to predict the transition point, and Head's method[10] is used for the turbulent portion.

From Michel's criteria, we are able to predict the transition point. In addition, the laminar separation point is located ahead of the transition point if

$$\lambda < -0.09 \tag{1}$$

Now we must check whether the boundary layer is reattached. From the bubble properties,[1] the length in the laminar portion of the bubble ℓ_1 is given by

$$\ell_1 = \frac{40{,}000\nu}{U_S} \tag{2}$$

and the bubble reattachment properties are

$$\lambda = -0.0059\, Re_\theta \tag{3}$$

$$H = 3.5 \tag{4}$$

$$\theta_R = \left[0.011233\frac{U_R}{U_s} - 0.003033\right]\ell_2 \Big/ \left(1 - \frac{U_R}{U_S}\right) \tag{5}$$

From Eqs. (3) and (5), the length of the bubble in the turbulent portion ℓ_2 can be obtained. During the calculation, three assumptions are made:

1) $U_T = U_S$, since the pressure is nearly constant in the laminar portion.

2) The velocity distribution is linear between the transition and reattachment points.

3) The velocity field outside the boundary layer is not apparently affected by bubble existence.

When the reattachment point is determined, Head's method is used for finding the turbulent separation point. As long as the value of the shape factor H falls between 1.8 and 2.4, turbulent separation is reached.

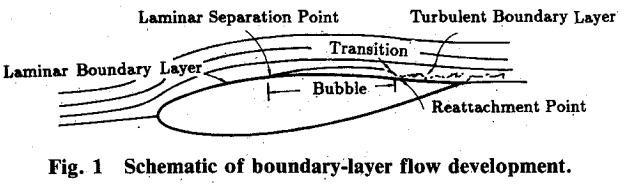

Fig. 1 Schematic of boundary-layer flow development.

Presented as Paper 88-2575 at the AIAA 6th Applied Aerodynamics Conference, Williamsburg, VA, June 6-8, 1988; received Nov. 25, 1988; revision received Feb. 10, 1989.

*Assistant Professor, Institute of Aeronautics and Astronautics. Member AIAA.

†Graduate Student, Institute of Aeronautics and Astronautics.

In order to obtain a preliminary prediction of the pressure distribution, the previous three assumptions and the plateau behavior of the pressure distribution after the turbulent separation point are employed to modify the pressure distribution from the panel method. These preliminary results are then compared to the experimental results[11] for two angles of attack (see Fig. 2). These comparisons for the laminar separation, the reattachment and the turbulent separation points on the upper surface are presented in Figs. 3 and 4. Although the preliminary predicted results agree with the experimental data in some cases, the C_p distributions at the leading edge and trailing edge portions are not as good as expected. In an effort to improve the numerical results, the following modification is introduced.

Vortex Wake Model

According to Sears' model[7] for a separated blunt trailing edge airfoil, as plotted in Fig. 5, the total change of circulation about the airfoil with two separation points A and B is given by

$$\frac{d\Gamma}{dt} = -\left(\frac{1}{2}U_A^2 - \frac{1}{2}U_B^2\right) \tag{6}$$

The strength of the vortices from the turbulent separation point at the upper surface of the airfoil is

$$\left(\frac{d\Gamma}{dt}\right)_S = -\frac{1}{2}U_S^2 \tag{7}$$

When the panel method is used, a series of singular points are deployed on the airfoil surface. This may interfere with the vortex wake model from which two other singular points are assigned. Thus, to modify the velocity at the separation point, one introduces

$$U_S = 0.25 \times \sum_{i=1}^{4} (U_i^2 + V_i^2)^{1/2} \tag{8}$$

The analyzed airfoils are NACA series airfoil 66_3-018 and 63_3-018. Their trailing edges are cusped and the velocity at the trailing edge has not been determined properly by numerical computation. In order to overcome this difficulty, Kelvin theorem

$$\frac{d\Gamma}{dt} = 0 \tag{9}$$

is introduced and expressed in numerical form as

$$\left(\Gamma_{\text{airfoil}}\right)^{k+1} + \Delta t\left(-\frac{1}{2}U_S^2\right)^{k+1} + \left(\Gamma_{\text{wake}}\right)^{k+1} = \left(\Gamma_{\text{airfoil}}\right)^{k} \tag{10}$$

where k is the iteration number.

The unknowns are the source strength on each panel, circulation strength about the airfoil, and the trailing edge vortex strength. The boundary conditions are the nopenetration condition on the control point of each panel and the Kelvin theorem. For the problem to be well posed, another boundary condition is needed. From the visualization study[11] about the airfoil, the flow direction leaving the lower surface of the trailig edge is geometrically tangent to its edge as long as the flow is separated somewhere on the upper surface. The pressure distribution C_p is obtained accordingly from

$$C_p = 1 - \frac{U_e^2}{U_\infty^2} - \frac{2}{U_\infty}\frac{\partial \phi}{\partial t} \tag{11}$$

The convergence criterion is set as in Eq. (12), and computation stops when $\epsilon < 10^{-4}$ or becomes periodic. The resultant C_p is then taken to be the time-averaged value of the final ten-period data.

$$\epsilon = \left| \frac{(\Gamma_{\text{airfoil}})^{k+1} - (\Gamma_{\text{airfoil}})^{k}}{(\Gamma_{\text{airfoil}})^{k}} \right| \leq 10^{-4} \tag{12}$$

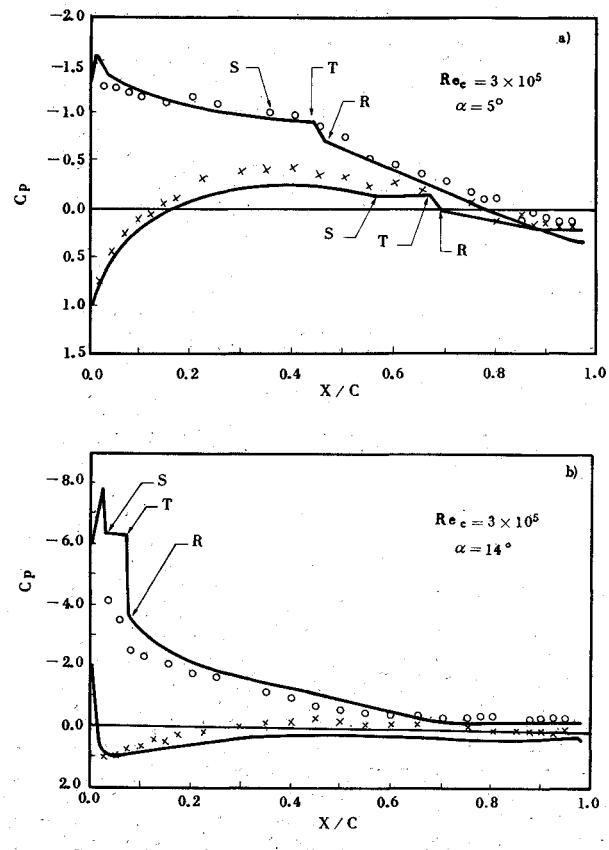

Fig. 2 Comparison of pressure distributions for preliminary prediction and experiment[11] for $Re_c = 3 \times 10^5$ at a) $\alpha = 5$ deg; b) $\alpha = 14$ deg.

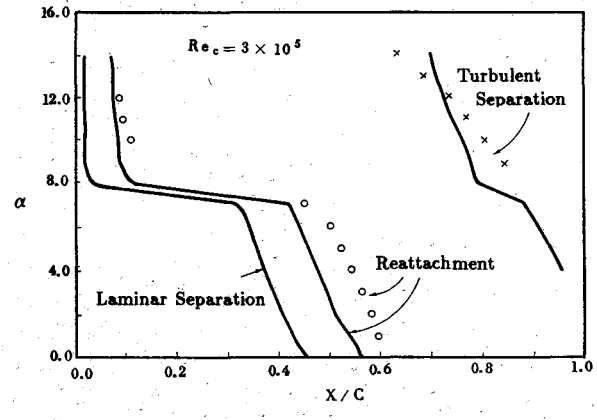

Fig. 3 Comparison of boundary-layer properties with angle of attack for $Re_c = 3 \times 10^5$ (– prediction; ○, × experiment[11]).

Results and Discussion

The comparison of the experimental C_p and the preliminary predicted C_p distributions show a plateau behavior in the bubble region and steeply decrease after. This confirms the

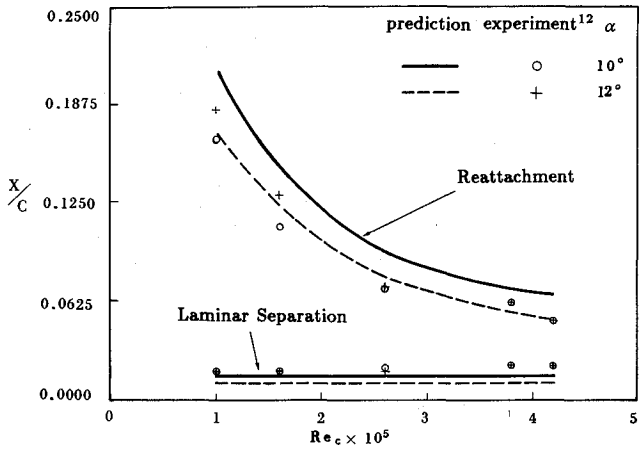

Fig. 4 Comparison of boundary-layer properties with Reynolds number for $\alpha = 10$ and 12 deg.

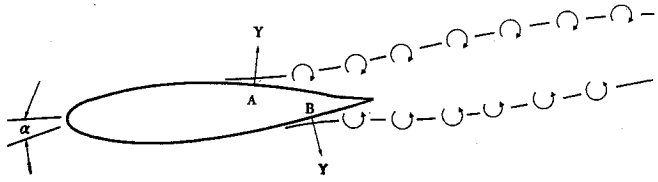

Fig. 5 The vortex wake model proposed by Sears.[7]

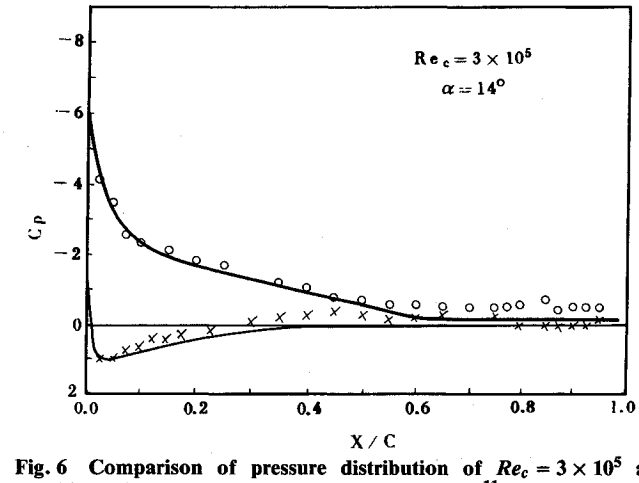

Fig. 6 Comparison of pressure distribution of $Re_c = 3 \times 10^5$ at $\alpha = 14$ deg (− present method; ○, × experiment[11]).

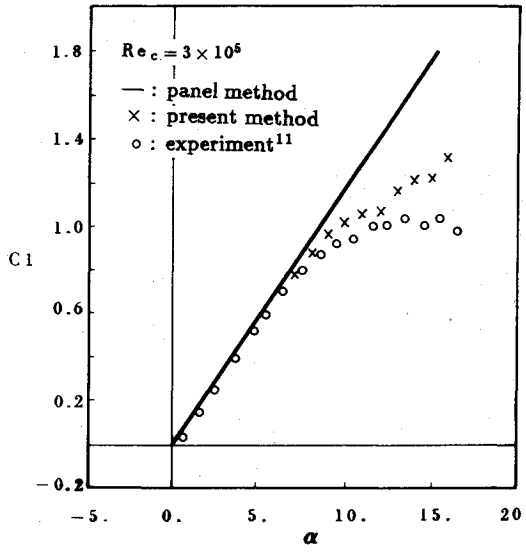

Fig. 7 Variation of lift coefficient with angle of attack for $Re_c = 3 \times 10^5$ (− panel method; × present method; ○ experiment[11]).

prediction calculation assumptions. For lower angle of attack, $\alpha = 5$ deg, the preliminary predicted C_p distributions clearly agree with the experiment, especially on the upper surface. However, for higher angles of attack, $\alpha = 14$ deg, the predicted results deviate more significantly from the experiment, and deteriorate badly at the leading and trailing edges, where the flow is separated and the wake occurs, respectively.

The predicted information about the boundary-layer properties are summarized in Fig. 3, along with the experiment[11] about NACA 63_3-018 airfoil for $Re_c = 3.0 \times 10^5$. The overall error is less than 10%. The predicted turbulent separation points will be utilized as the vortex-releasing points in the vortex wake model, where the C_p distributions will be modified accordingly. Figure 4 also shows the prediction of bubble formation for NACA 66_3-018 airfoil[12] at $\alpha = 10$ and 12 deg, with respect to the Reynolds number. Although some of the errors may be as high as 30%, a satisfactory comparison also exists here.

Figure 6 shows the result of the computation by the vortex wake model with further modification. The C_p distribution calculated here is improved in comparison with the previous preliminary result and agrees quite well with the experimental data, particularly in the front portion of the airfoil. Figure 7 illustrates the comparison of the lift coefficient C_l for the solution by panel method, modified solution with wake model, and experiment at various angles of attack. It is apparent that there is a substantial improvement between the modified solution and the panel method solution, especially after the linear region in the lift curve.

Concluding Remarks

A simplified procedure is developed for predicting the aerodynamic parameters and bubble formation on NACA series airfoils in the low Reynolds number range. The modified scheme with vortex wake model demonstrates good agreement with experimental data. In addition, only 20 s per case of VAX-8600 CPU time is required for the preliminary prediction calculation, whereas it takes about 12 min per case for the modified solution calculation. The procedure is quite efficient and suitable for practical application.

References

[1]Horton, H. P., "Laminar Separation Bubbles in Two and Three Dimensional Incompressible Flow," Ph.D. Dissertation, Univ. of London, England, 1968.

[2]Roberts, W. B., "Calculation of Laminar Separation Bubbles and their Effect on Airfoil Performance," *AIAA Journal*, Vol. 18, Jan. 1980, pp. 25-31.

[3]Cotton, F. N. and Galbraith, R. A., "A Simple Method for the Prediction of Separation Bubble Formation on Airfoil at Low Reynolds Number," *Proceedings of Conference on Low Reynolds Number*, The Royal Aeronautical Society, London, England, Vol. 1, Oct. 1986, pp. 3.1-3.17.

[4]Basu, B. C and Hancock, G. J., "The Unsteady Motion of a Two-Dimensional Aerofoil in Incompressible Inviscid Flow," *Journal of Fluid Mechanics*, Vol. 87, Part 1, July 1978, pp. 157-178.

[5]Kim, M. J. and Mook, D. T., "Application of Continuous Vorticity Panels to General Unsteady Incompressible Two-Dimensional Lifting Flow," *Journal of Aircraft*, Vol. 23, June 1986, pp. 464-471.

[6]Katz, J., "A Discrete Vortex Method for the Nonsteady Separated Flow over an Airfoil," *Journal of Fluid Mechanics*, Vol. 102, Jan. 1981, pp. 315-328.

[7]Sears, W. R., "Unsteady Motion of Airfoils with Boundary-Layer Separation," *AIAA Journal*, Vol. 14, Feb. 1976, pp. 216-220.

[8]Blaslovich, J. D., "A Comparison of Separated Flow Airfoil Analysis Methods," *Journal of Aircraft*, Vol. 22, March 1985, pp. 208-214.

[9]Moran, J., *An Introduction to Theoretical and Computational Aerodynamics*, Wiley, New York, 1984, pp. 221-222.

[10]Cebeci, T. and Bradshaw, P., *Momentum Transfer in Boundary Layers*, McGraw-Hill, New York, 1977, pp. 108-114, 192-197.

[11]Hsiao, F. B., Liu, C. F., and Tang, Z., "Aerodynamic Performance and Flow Structure Studies of a Low Reynolds Number Airfoil," Vol. 27, Feb. 1989, pp. 129-137.

[12]Mueller, T. J. and Batill, S. M., "Experimental Studies of the Laminar Separation Bubble on a Two-Dimensional Airfoil at Low Reynolds Numbers," AIAA Paper 80-1440, July 1980.

Numerical Simulation of Aircraft Rotary Aerodynamics

Joseph Katz*
San Diego State University, San Diego, California

Introduction

AERODYNAMIC load evaluation for aircraft maneuvers such as the coning motion is much needed during the development process of modern fighter aircraft. Such aerodynamic data can be obtained by rotary-rig experiments, which can simulate aircraft coning and spinning conditions.[1-3] Because of the complex nature of this type of testing, the number of facilities having rotary rigs in their wind tunnels is small. Additionally, the experimental data reduction process must account for effects such as model dynamics, wind-tunnel blockage, and model mounting interference.[3] Computational simulation of these aircraft maneuvers can complement the experimental determination of the aerodynamic coefficients and, thereby, accelerate vehicle development process.

In the present study, a three-dimensional panel model for a generic fighter airplane (Standard Dynamic Model,[1,2] or SDM) was prepared, and its capability of simulating the three-dimensional coning motion was investigated.

Contents

The numerical scheme used here is based on a three-dimensional potential-flow method combined with a time-dependent vortex wake model to simulate the shear layers emanating from the trailing edges of lifting surfaces. The baseline code[4] uses quadrilateral panel lattice with piecewise constant doublet and source surface elements. This approach was widely used before[5] for steady-state, high Reynolds number, lifting, nonseparated, and subsonic flows. For this case of coning motion, the spiral wake behind the airplane is constructed by the time-stepping method. The motion begins with a "no-wake" condition, and for the case of coning motion will evolve until the starting-vortex effect on the solution becomes negligible (about one complete revolution for $\omega b/2U<0.05$). More details about the methodology and the particular formulation used here are provided in Ref. 4.

For this preliminary study of modeling the coning motion, the SDM was presented by 718 panels, and its geometry is shown in the inset of Fig. 1. More detailed dimensions of the model are provided in Refs. 9-11. Since the experimental data of Refs. 1 and 2 were taken at a Mach number M of 0.6, the effect of compressibility was investigated briefly by conducting a lower-speed static test (at $M=0.15$) with a similar model. The results of this test, and the normal force C_z data of Ref. 1, is compared with the computed results in Fig. 1. At the lower angles of attack ($\alpha<15$ deg), the computed curve falls close to the two sets of experimental data, but a closer inspection reveals that the low-speed data are slightly lower than the high-speed data (as predicted by the Prandtl-Glauert law). The wing's leading-edge sweep is only 40 deg and, therefore, at this angle-of-attack range, wing leading-edge separation will not dominate the lift characteristics. However, at angles of attack over 25 deg, the flow separation from the strakes intensifies and increases the experimental lift coefficients over the computed ones. This effect of strake vortex flow, which seems to cause larger C_z in the $M=0.15$ tests, was not modeled numerically here. Based on this normal force data of Fig. 1, and because of the low reduced frequencies in the experiments of Refs. 1 and 2, it is assumed that compressibility effects are small and fall within the limits predicted by the Prandtl-Glauert law.

Computed and experimental side force C_y and rolling moment C_ℓ are presented in Figs. 2 and 3, and the parameters such as angle-of-attack α and rotation rate ω for the coning motion are described in the inset to Fig. 2. For this case, the aircraft was rotated about its center of gravity at a rate of

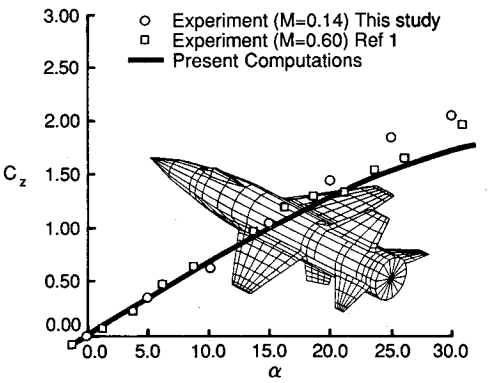

Fig. 1 Normal force coefficient vs angle of attack and geometry of the Standard Dynamic Model (SDM).

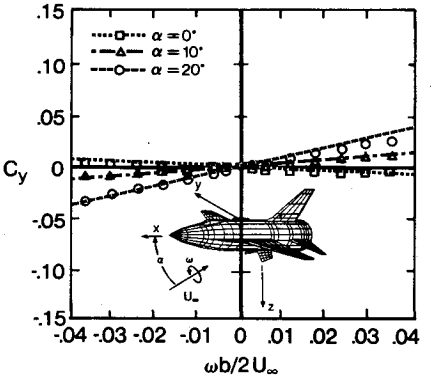

Fig. 2 Side force C_y vs roll rate $\omega b/2U_\infty$ for the SDM, and description of the coning motion.

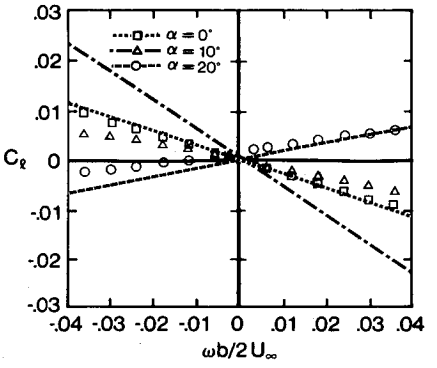

Fig. 3 Rolling moment C_ℓ vs roll rate $\omega b/2U_\infty$ for the SDM.

Presented as Paper 88-0399 at the AIAA 26th Aerospace Sciences Meeting, Reno, NV, Jan. 11-14, 1988; received April 27, 1988; revision received Nov. 18, 1988.

*Professor, Department of Aerospace Engineering.